

## Low-energy electron-impact single ionization of helium

J. Colgan,<sup>1</sup> M. S. Pindzola,<sup>2</sup> G. Childers,<sup>3</sup> and M. A. Khakoo<sup>3</sup>

<sup>1</sup>*Theoretical Division, Los Alamos National Laboratory, Los Alamos, New Mexico 87545, USA*

<sup>2</sup>*Department of Physics, Auburn University, Auburn, Alabama 36849, USA*

<sup>3</sup>*Department of Physics, California State University, Fullerton, California 92834, USA*

(Received 1 February 2006; published 18 April 2006)

A study is made of low-energy electron-impact single ionization of ground-state helium. The time-dependent close-coupling method is used to calculate total integral, single differential, double differential, and triple differential ionization cross sections for impact electron energies ranging from 32 to 45 eV. For all quantities, the calculated cross sections are found to be in very good agreement with experiment, and for the triple differential cross sections, good agreement is also found with calculations made using the convergent close-coupling technique.

DOI: [10.1103/PhysRevA.73.042710](https://doi.org/10.1103/PhysRevA.73.042710)

PACS number(s): 34.80.Dp

### I. INTRODUCTION

The study of electron-impact single ionization of light atoms has proven a rich source for advances in the understanding of the subtle electron dynamics between two outgoing electrons. The effects of these electron-electron correlations are often most pronounced in studies of differential cross sections (in angle and/or in energy) between the outgoing electrons. However, the total integral ionization cross section is also an important quantity since this measures the flux of electrons from the ionization process and so is critical in the determination of absolute differential cross sections.

Subsequently, much effort has been focused on the electron-impact ionization of the two lightest atoms, hydrogen and helium. For hydrogen, measurements of the total integral ionization cross section made almost 20 years ago [1] still provide a benchmark for theory, and in the past 15 years several nonperturbative calculations [2–5] have demonstrated good agreement with these measurements. In more recent years, some of these theoretical methods have shown very good agreement with each other and with experimental measurements of the single and triple differential cross sections for this process [6–8], and also for the double differential cross sections at low impact energy [9,10].

For ground-state helium, accurate experimental measurements for the total integral single ionization cross sections are available [11,12], which are in good agreement with recent theoretical calculations [13]. Several detailed experimental and theoretical studies of the differential cross sections arising from this single ionization process have also been made recently [14–16], with impressively good agreement demonstrated very recently between experiment and theory [17]. It appears that the now good agreement between the latest calculations and measurements of the differential cross sections, demonstrated for the differential cross sections arising from the electron-impact ionization of hydrogen, is being extended to the ionization of ground-state helium.

We present in this paper a comprehensive study of the total integral, single, double, and triple differential cross sections for the electron-impact single ionization of ground-state helium at moderately low impact energies, using the time-dependent close-coupling (TDCC) method. Good agreement is found in nearly all cases between theory and available experimental measurements. We also compare with recent convergent close-coupling calculations [17,18] where good agreement is also found for most comparisons. We note that this work extends previous studies of the electron-impact single ionization of helium using the TDCC method [13], where good agreement was found between TDCC and experimental measurements of the total integral and single differential ionization cross sections. The TDCC method has also been used recently to calculate the total integral electron-impact double ionization cross section for helium [19] by extending our method to fully include the interactions between three outgoing electrons.

### II. THEORY

For low-energy electron-impact single ionization of ground-state helium, we “freeze” one of the inner  $1s$  electrons since it will take no part in the ionization process in this energy range. At much higher energies however, where the  $\text{He}^+$  ion may be left in an excited state after single ionization, or where double ionization is possible, the interactions of this electron must be fully taken into account [19].

The time-dependent Schrödinger equation for the two active electrons can then be written as

$$i \frac{\partial \Psi(\vec{r}_1, \vec{r}_2, t)}{\partial t} = H(\vec{r}_1, \vec{r}_2) \Psi(\vec{r}_1, \vec{r}_2, t), \quad (1)$$

where the time-independent Hamiltonian is given by

$$H(\vec{r}_1, \vec{r}_2) = -\frac{1}{2} \nabla_1^2 - \frac{1}{2} \nabla_2^2 - \frac{Z}{r_1} - \frac{Z}{r_2} + \frac{1}{|\vec{r}_1 - \vec{r}_2|} + V(r_1) + V(r_2), \quad (2)$$

where in this case  $Z=2$ . The total wave function for the two active electrons may be expanded in coupled spherical harmonics and projected onto the time-dependent Schrödinger equation to obtain the following set of partial differential equations for each  $LS$  symmetry:

$$i \frac{\partial P_{l_1 l_2}^{LS}(r_1, r_2, t)}{\partial t} = T_{l_1 l_2}(r_1, r_2) P_{l_1 l_2}^{LS}(r_1, r_2, t) + \sum_{l'_1 l'_2} U_{l_1 l_2, l'_1 l'_2}^L(r_1, r_2) P_{l'_1 l'_2}^{LS}(r_1, r_2, t), \quad (3)$$

where

$$T_{l_1 l_2}(r_1, r_2) = -\frac{1}{2} \frac{\partial^2}{\partial r_1^2} - \frac{1}{2} \frac{\partial^2}{\partial r_2^2} + \frac{l_1(l_1+1)}{2r_1^2} + \frac{l_2(l_2+1)}{2r_2^2} - \frac{Z}{r_1} + V_D(r_1) + V_X(r_1) - \frac{Z}{r_2} + V_D(r_2) + V_X(r_2) \quad (4)$$

and the coupling operator is given by

$$U_{l_1 l_2, l'_1 l'_2}^L(r_1, r_2) = (-1)^{L+l_2+l'_2} \sqrt{(2l_1+1)(2l'_1+1)(2l_2+1)(2l'_2+1)} \times \sum_{\lambda} \frac{r_{\leq}^{\lambda}}{r_{>}^{\lambda+1}} \begin{pmatrix} l_1 & \lambda & l'_1 \\ 0 & 0 & 0 \end{pmatrix} \begin{pmatrix} l_2 & \lambda & l'_2 \\ 0 & 0 & 0 \end{pmatrix} \begin{Bmatrix} L & l'_2 & l'_1 \\ \lambda & l_1 & l_2 \end{Bmatrix}. \quad (5)$$

In this equation, the “direct” potential terms are given by

$$V_D(r) = \int_0^{\infty} \frac{P_{1s}^2(r_1)}{\max(r_1, r)} dr_1 \quad (6)$$

and act to shield the outer active electrons from the full Coulomb attraction of the nucleus. The “frozen-core” radial orbital  $P_{1s}(r)$  is calculated as the hydrogenic ground-state radial orbital of  $\text{He}^+$ . A set of single-particle radial orbitals  $\bar{P}_{nl}(r)$  are then obtained by diagonalization of the single-particle Hamiltonian given by

$$h(r) = -\frac{1}{2} \frac{\partial^2}{\partial r^2} + \frac{l(l+1)}{2r^2} - \frac{Z}{r} + V_D(r) + V_X(r), \quad (7)$$

where in this case the “exchange” potential  $V_X(r)$  is calculated using a semiempirical local potential [20],

$$V_X(r) = -\alpha \left( \frac{24\rho_{1s}(r)}{\pi} \right)^{1/3}, \quad (8)$$

where  $\alpha$  is an adjustable parameter and  $\rho_{1s}(r) = P_{1s}^2/4\pi r^2$  is the radial probability density of the core electron. The  $\bar{P}_{nl}(r)$  radial orbitals are very similar to the Hartree-Fock radial orbitals of He.

The two-electron radial functions of Eq. (3) at time  $t=0$  are constructed as

$$P_{l_1 l_2}^{LS}(r_1, r_2, t=0) = \sqrt{\frac{1}{2}} \left[ G_{k_1 l_1}(r_1) \delta_{0, l_2} \bar{P}_{1s}(r_2) + (-1)^S \delta_{0, l_1} \bar{P}_{1s}(r_1) G_{k_2 l_2}(r_2) \right], \quad (9)$$

where  $k$  is the linear momentum and  $G_{kl}(r)$  is a radial wave packet. The coupled equations (3) are then propagated according to the usual time-dependent close-coupling prescription, for each  $LS$  symmetry. At an appropriate time  $t=T$  after the collision, in which only outgoing waves are present in each channel, the wave function in momentum space for each  $LS$  symmetry is given by

$$P_{l_1 l_2}^{LS}(k_1, k_2) = \int \int P_{k_1 l_1}(r_1) P_{k_2 l_2}(r_2) P_{l_1 l_2}^{LS}(r_1, r_2, t=T) dr_1 dr_2, \quad (10)$$

where  $P_{kl}(r)$  are single-particle continuum channels that are appropriately normalized as

$$P_{kl}(r) \rightarrow \sqrt{\Delta k} \sin \left( kr + \frac{q}{k} \ln(2kr) - \frac{l\pi}{2} + \sigma_l + \delta_l \right), \quad (11)$$

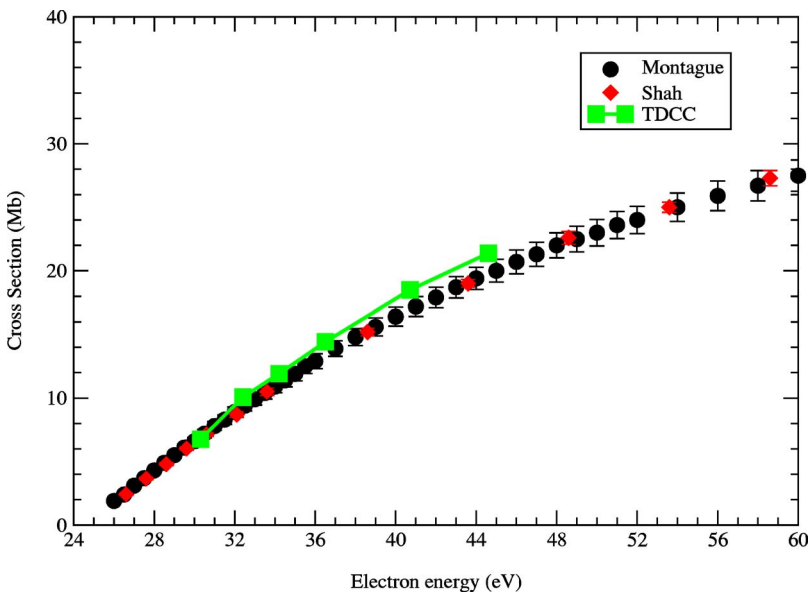


FIG. 1. (Color online) Total electron-impact single ionization cross section for He. The theoretical time-dependent close-coupling calculations (squares) are compared with previous expt. measurements of Montague *et al.* [11] and Shah *et al.* [12] ( $1.0 \text{ Mb} = 1.0 \times 10^{-18} \text{ cm}^2$ ).

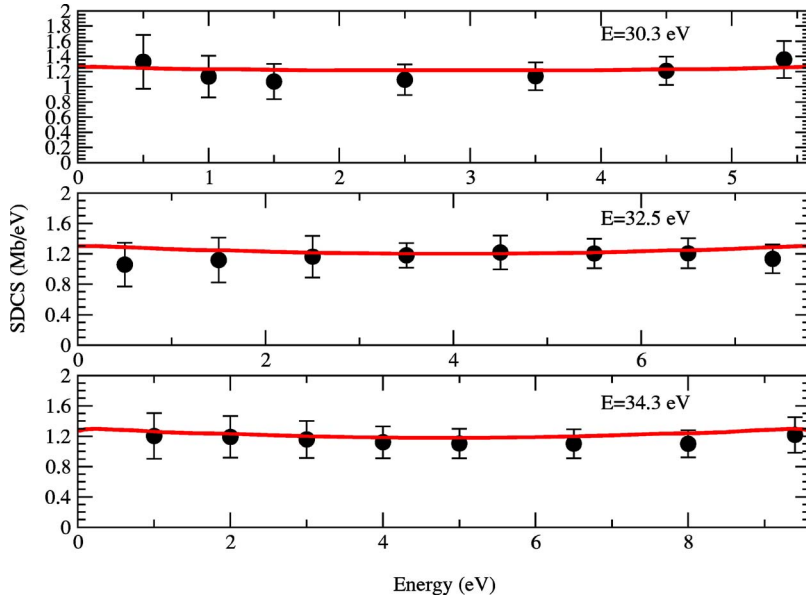


FIG. 2. (Color online) Single differential cross sections for helium at incident electron energies of 30.3, 32.5, and 34.3 eV, as a function of the ejected electron energy. The solid lines are time-dependent close-coupling calculations, and the solid circles are expt. measurements [18] ( $1.0 \text{ Mb} = 1.0 \times 10^{-18} \text{ cm}^2$ ).

where  $\sigma_l$  is the Coulomb phase shift,  $\delta_l$  is the distorted-wave phase shift,  $\Delta k$  is the momentum mesh spacing, and  $q$  is the asymptotic charge.

This momentum space wave function allows us to simply define the differential cross sections. The triple differential cross section is given by

$$\begin{aligned} \frac{d^3\sigma}{d\alpha d\Omega_1 d\Omega_2} &= \frac{\pi}{4k^2} \sum_S (2S+1) \frac{2}{\pi} \int dk_1 \frac{2}{\pi} \int dk_2 \\ &\times \delta\left(\alpha - \tan^{-1}\left[\frac{k_2}{k_1}\right]\right) \left| \sum_L i^L \sqrt{2L+1} \right. \\ &\times \sum_{l_1 l_2} (-i)^{l_1+l_2} e^{i(\sigma_{l_1}+\sigma_{l_2})} e^{i(\delta_{l_1}+\delta_{l_2})} P_{l_1 l_2}^{LS}(k_1, k_2) \\ &\times \sum_{m_1, m_2} C_{m_1 m_2 0}^{l_1 l_2 L} Y_{l_1 m_1}(\hat{k}_1) Y_{l_2 m_2}(\hat{k}_2) \left. \right|^2, \quad (12) \end{aligned}$$

where in this case  $\alpha$  is the angle in the hyperspherical plane between the two outgoing momenta vectors  $k_1$  and  $k_2$ ,  $Y_{lm}(\hat{k})$  is a spherical harmonic, and  $C_{m_1 m_2 m_3}^{l_1 l_2 l_3}$  is a Clebsch-Gordan coefficient. The double differential cross section in angle is obtained by integrating the triple differential cross section over one of the outgoing electron angles  $\Omega$ . The single differential cross section is given by

$$\begin{aligned} \frac{d\sigma}{d\alpha} &= \frac{\pi}{4k^2} \sum_{L,S} (2L+1)(2S+1) \frac{2}{\pi} \int dk_1 \frac{2}{\pi} \int dk_2 \\ &\times \delta\left(\alpha - \tan^{-1}\left[\frac{k_2}{k_1}\right]\right) \sum_{l_1 l_2} |P_{l_1 l_2}^{LS}(k_1, k_2)|^2, \quad (13) \end{aligned}$$

$$\frac{d\sigma}{dE_1} = \frac{1}{k_1 k_2} \frac{d\sigma}{d\alpha} \quad (14)$$

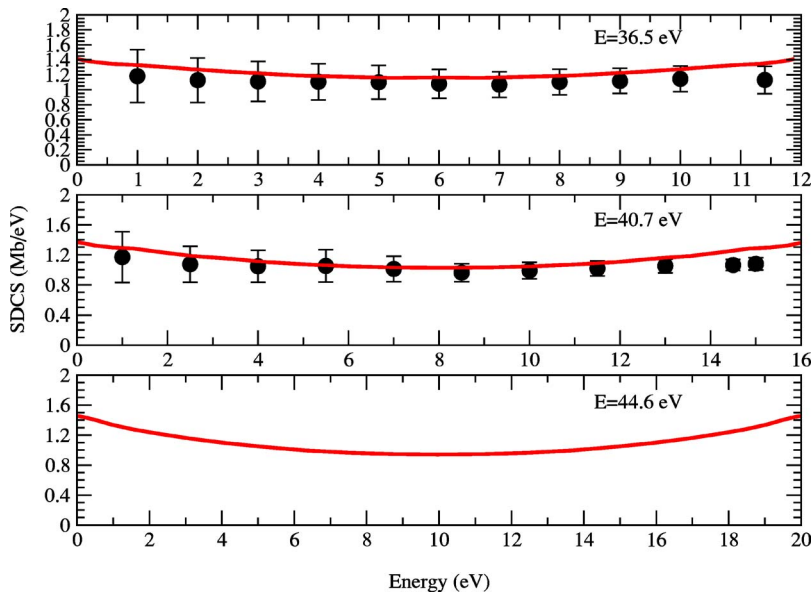


FIG. 3. (Color online) Single differential cross sections for helium at incident electron energies of 36.5, 40.7, and 44.6 eV, as a function of the ejected electron energy. The solid lines are time-dependent close-coupling calculations, and the solid circles are the expt. measurements [18] ( $1.0 \text{ Mb} = 1.0 \times 10^{-18} \text{ cm}^2$ ).

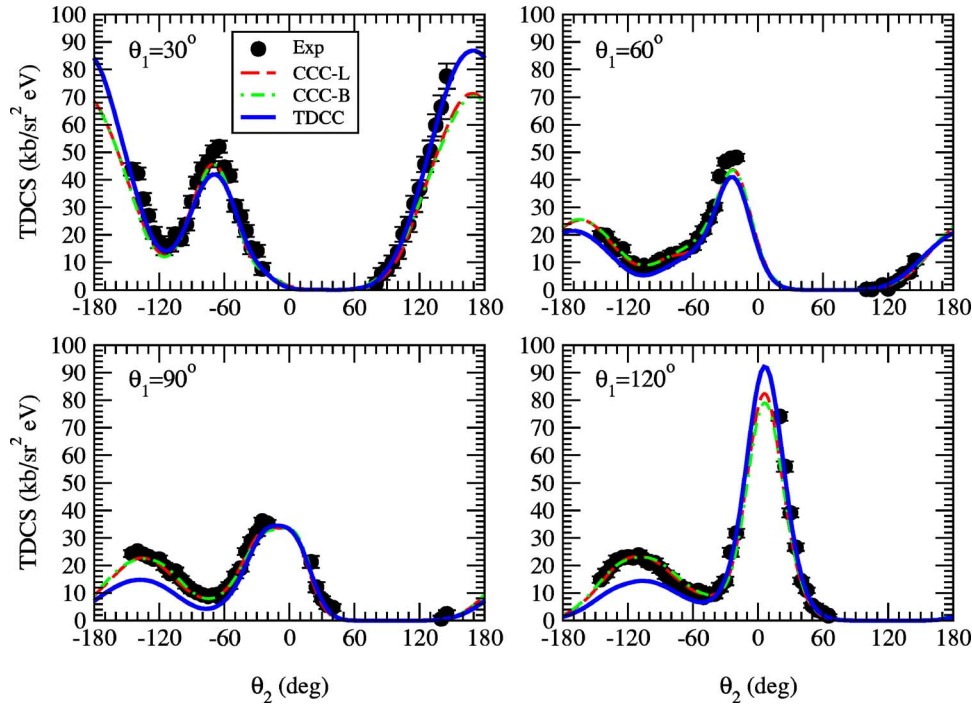


FIG. 4. (Color online) Triple differential cross sections for helium at an incident electron energy of 44.6 eV, for various angles of one of the ejected electrons, as indicated. The excess energy is equally shared between the two electrons, i.e.,  $E_1 = E_2 = 10$  eV. The new time-dependent close-coupling calculations are compared with the expt. measurements of Rioual *et al.* [16] and two sets of convergent close-coupling calculations (CCC-L and CCC-B) of Stelbovics *et al.* [17] ( $1.0 \text{ kb} = 1.0 \times 10^{-21} \text{ cm}^2$ ).

and the total integral ionization cross section is then

$$\sigma = \int_0^{\pi/2} \frac{d\sigma}{d\alpha} d\alpha = \int_0^E \frac{d\sigma}{dE_1} dE_1, \quad (15)$$

where the ejected energy  $E_1 = k_1^2/2$  and the total energy  $E = k_1^2/2 + k_2^2/2$ .

### Results

Our time-dependent close-coupling calculations were carried out using a mesh spacing of  $\Delta r = 0.2$  a.u. and with box sizes ranging from 96 to 144 a.u. Larger box sizes were found to be necessary to fully converge the triple differential cross sections, which, of all the quantities presented here,

were found to have the slowest convergence properties. Also, the number of  $LS$  symmetries used varied from  $L=6$  to 10, with more symmetries required at larger incident energies in order to fully converge the differential cross sections. The convergence of the differential cross sections for individual  $LS$  symmetries was also monitored as a function of the number of  $l_1 l_2$  pairs included in the calculation.

We begin our discussion of the single ionization of the ground state of helium by examining the total integral ionization cross section. Our TDCC calculation from incident energies of 30–45 eV is shown in Fig. 1 and compared with the experimental measurements of Montague *et al.* [11] and Shah *et al.* [12]. Good agreement is found between our calculations and the experimental measurements. We note that previous TDCC calculations have also demonstrated good

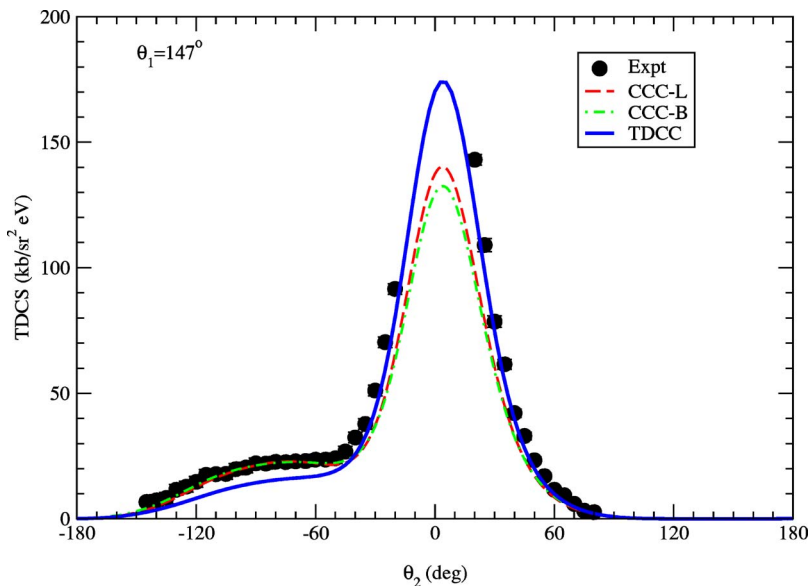


FIG. 5. (Color online) Same as Fig. 4, for an ejected electron angle of 147 degrees.

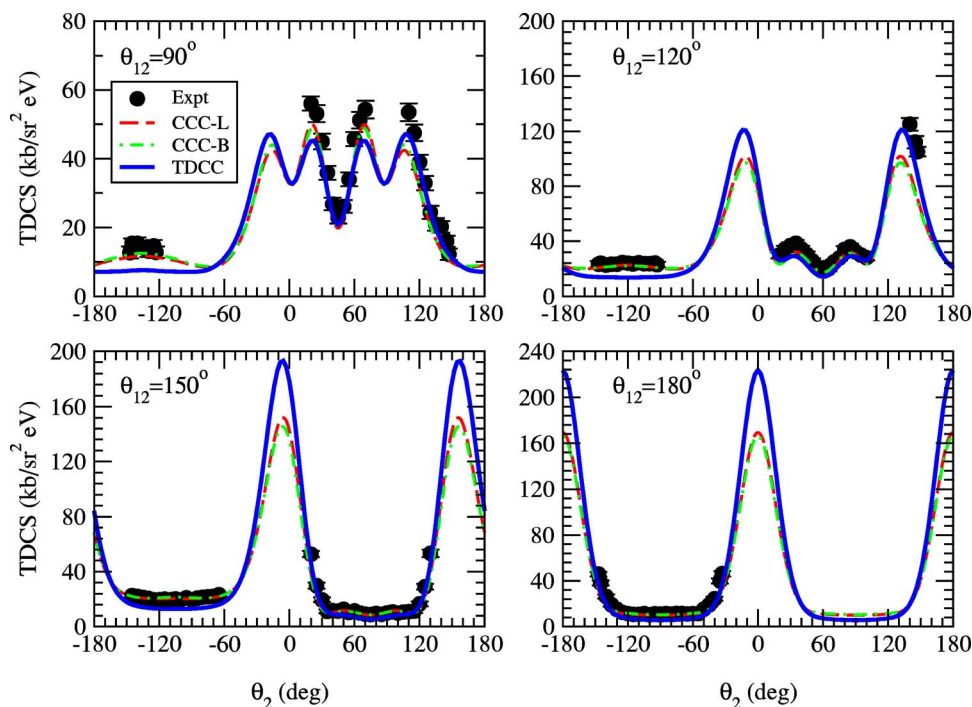


FIG. 6. (Color online) Same as Fig. 4, for four cases where the angle between the ejected electrons ( $\theta_{12}$ ) is held fixed as indicated.

agreement at much higher impact energies around the peak of the cross section [13].

In Figs. 2 and 3, we present single differential cross sections in energy for six different impact energies. Our TDCC calculations are compared with very recent experimental measurements [18]. In this case, excellent agreement is found between the measurements and the TDCC calculations at lower incident energies. At the incident energy of 40.7 eV, there is a small but statistically significant disagreement at the highest energies of the ejected electron. As expected, the TDCC single differential cross sections become somewhat more “smile-shaped” as the incident energy is increased. Although this trend is difficult to discern in the experimental measurements, the TDCC calculations fall, for the most part, very near the experimental points, and in almost all cases, well within the experimental error bars.

We now turn to a comparison of the triple differential cross section. In this case, we compare our calculations at an incident energy of 44.6 eV with the recent measurements of Rioual *et al.* [16] and the most recent sets of convergent close-coupling (CCC) calculations [17]. Two sets of CCC calculations, one using a Laguerre basis (CCC-L) and one using box-based target functions (CCC-B), are shown. Figures 4 and 5 show the triple differential cross section at equal energy sharing between the outgoing electrons for various fixed values of  $\theta_1$ , the angle of the first ejected electron. We find that the TDCC results are in very good agreement with the experimental measurements and, for the most part, with the CCC calculations. The peaks of the TDCC cross sections are generally larger than the peaks of the CCC calculations, although in all cases, the shapes of the cross sections are in excellent agreement between the two theories. For large

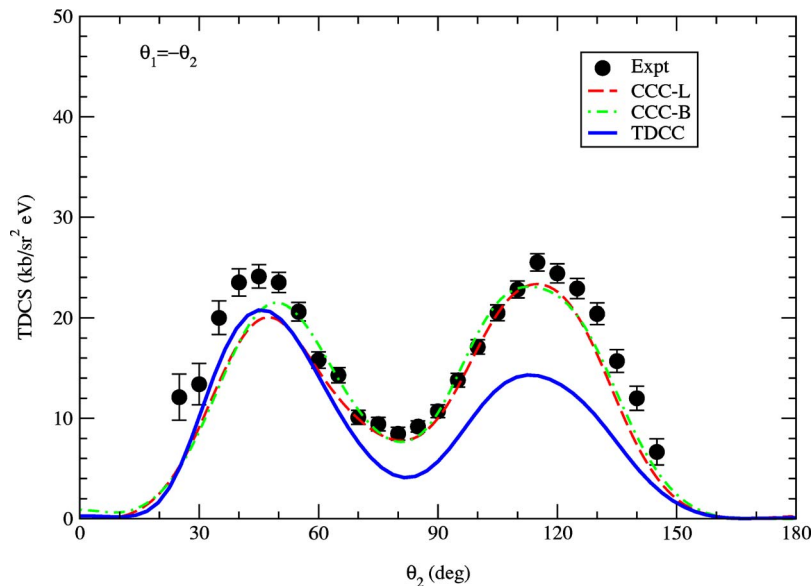


FIG. 7. (Color online) Same as Fig. 4, where in this case the cross section is measured such that the angle of one of the ejected electrons is equal to the angle of the other ejected electron, but on a different side of the scattering plane ( $\theta_1 = -\theta_2$ ).

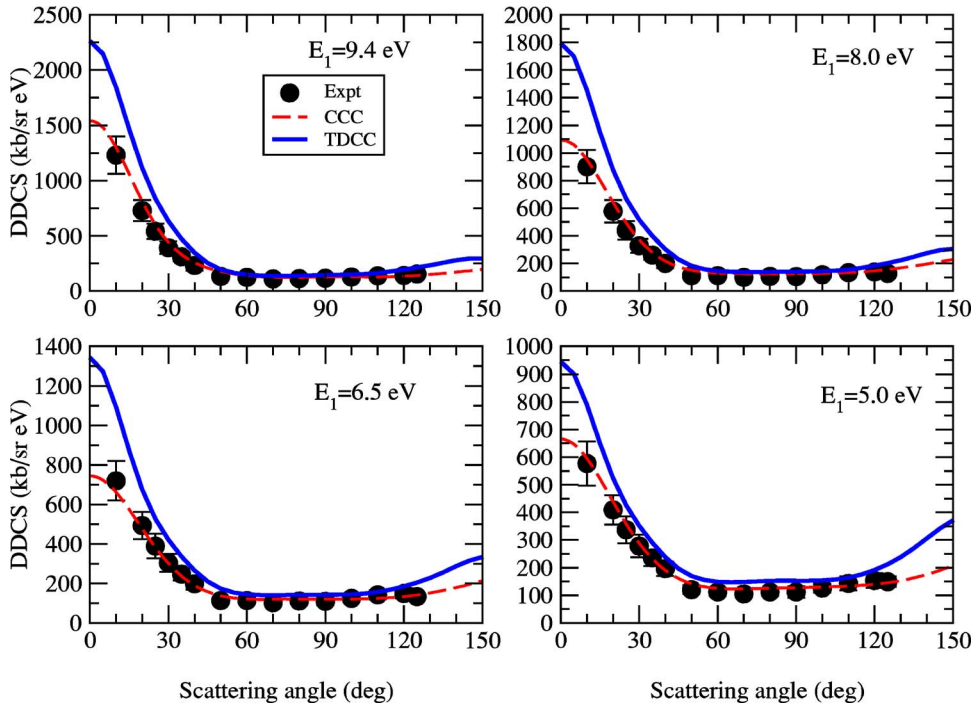


FIG. 8. (Color online) Double differential cross sections for helium at an incident electron energy of 34.3 eV, as a function of one of the ejected electron's energy and ejected angle. We compare with expt. measurements [18] and with convergent close-coupling calculations [18] ( $1.0 \text{ kb} = 1.0 \times 10^{-21} \text{ cm}^2$ ).

negative values of  $\theta_2$ , our calculations are slightly lower than experiment, but for the forward scattering angles, TDCC and experiment are in excellent agreement. We note that, unlike [17], we have not scaled the experimental measurements in these figures, although we do note that the measurements [16] quote an absolute uncertainty of 25%.

In Figs. 6 and 7 we compare with the same set of measurements and CCC calculations for cases where the angle between the ejected electrons ( $\theta_{12}$ ) is held fixed, again for the case where the energy is shared equally between the out-

-going electrons. Again, for the most part, very good agreement is seen between the TDCC calculations and the measurements. Also, the CCC calculations are generally in good agreement with the TDCC calculations, with again TDCC predicting a larger peak in the triple differential cross section than CCC. In Fig. 7 (the case where  $\theta_1 = -\theta_2$ ), the TDCC calculations are in fairly poor agreement at larger values of  $\theta_2$ . The TDCC cross section is also not symmetric, unlike the measurements and the CCC calculations. The reasons for this are unclear; these calculations were made using exactly the

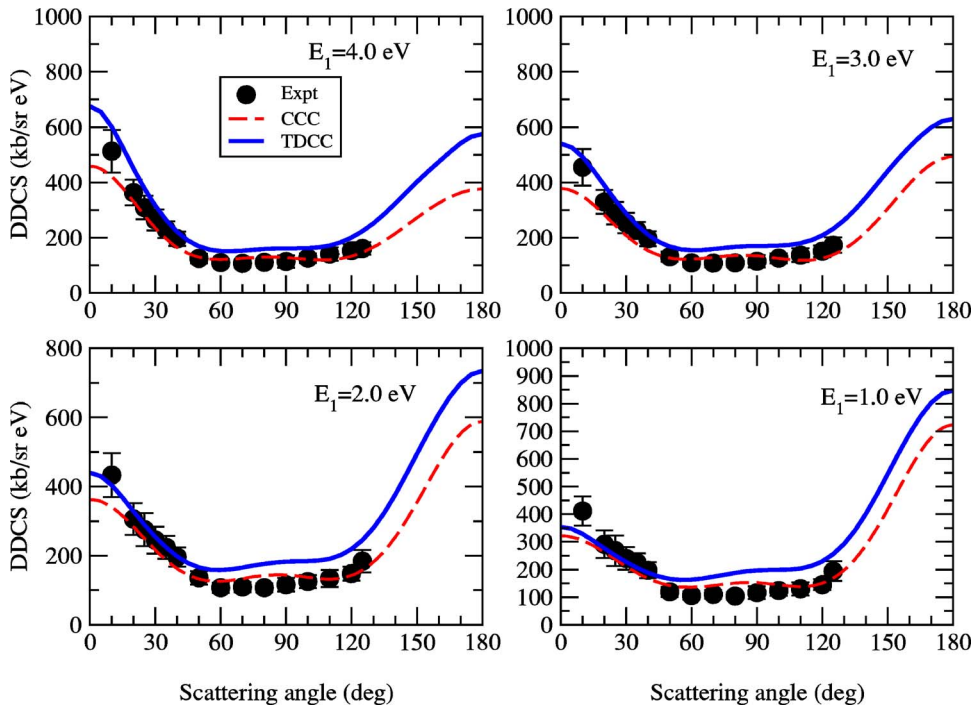


FIG. 9. (Color online) Same as Fig. 8, for more values of the first ejected electron's energy.

same methods as the previous figures. We again note that we have not scaled the experimental measurements in any of these figures.

Finally, in Figs. 8 and 9 we present double differential cross sections for the electron-impact ionization of helium at an incident energy of 34.3 eV, for various values of the energy of the first electron  $E_1$ . Again we compare with recent experimental measurements [18]. We also have recent CCC calculations with which to compare [18]. In this case, the agreement between TDCC and experimental measurement is generally good. For the most part, the TDCC calculations fall within the experimental error bars, with the exception of the highest values of  $E_1$ , where we again see the pattern that the TDCC calculations peak at a higher value than the CCC calculations. At lower values of  $E_1$  the TDCC calculations are in very good agreement with the experimental measurements, especially at the lower angles  $\theta_1$ . In all cases, the shapes of the double differential cross sections predicted by experiment are very well reproduced by both theoretical calculations.

### III. SUMMARY

In this paper, we have made a study of the low-energy electron-impact single ionization of ground-state helium. We have made detailed calculations using the time-dependent close-coupling method of total integral ionization cross sections, and all possible differential cross sections. We have compared, where available, with the most recent experimen-

tal measurements, and other state-of-the-art theoretical calculations. For the majority of cases, the TDCC calculations are in excellent agreement with experiment, for a wide range of differential and integral cross sections. Very good agreement has also been demonstrated between TDCC and calculations using the CCC method. However, the agreement is not perfect by any means. Although we are confident that our TDCC calculations are well converged with respect to the several possible convergence parameters inherent in our calculations (i.e., box size, number of  $l_1 l_2$  pairs for a given  $LS$  symmetry, and total number of  $LS$  symmetries included), it remains to be seen whether differences between calculations, and with experiment, are due to some lack of convergence in any of the calculations, or to more subtle effects. It is hoped that more extensive calculations and further studies will further improve the agreement shown here. We also plan to examine the differential cross sections arising from the electron-impact ionization of other light species, in our continuing efforts to explore the subtle dynamics arising from the correlated motion of two electrons moving in a Coulomb field.

### ACKNOWLEDGMENTS

We thank I. Bray for communication of his results in numerical form. A portion of this work was performed under the auspices of the U.S. Department of Energy through the Los Alamos National Laboratory, and a grant to Auburn University. Computational work was performed on the BPROC machines at Los Alamos National Laboratory.

- 
- [1] M. B. Shah, D. S. Elliott, and H. B. Gilbody, *J. Phys. B* **20**, 3501 (1987).
  - [2] I. Bray and A. T. Stelbovics, *Phys. Rev. Lett.* **70**, 746 (1993).
  - [3] D. Kato and S. Watanabe, *Phys. Rev. Lett.* **74**, 2443 (1995).
  - [4] K. Bartschat and I. Bray, *J. Phys. B* **29**, L577 (1996).
  - [5] M. S. Pindzola and F. Robicheaux, *Phys. Rev. A* **54**, 2142 (1996).
  - [6] I. Bray, *J. Phys. B* **33**, 581 (2000).
  - [7] T. N. Rescigno, M. Baertschy, W. A. Isaacs, and C. W. McCurdy, *Science* **286**, 2474 (1999).
  - [8] J. Colgan, M. S. Pindzola, F. J. Robicheaux, D. C. Griffin, and M. Baertschy, *Phys. Rev. A* **65**, 042721 (2002).
  - [9] J. G. Childers, K. E. James, M. Hughes, I. Bray, M. Baertschy, and M. A. Khakoo, *Phys. Rev. A* **68**, 030702(R) (2003).
  - [10] J. G. Childers, K. E. James, I. Bray, M. Baertschy, and M. A. Khakoo, *Phys. Rev. A* **69**, 022709 (2004).
  - [11] R. G. Montague, M. F. A. Harrison, and A. C. H. Smith, *J. Phys. B* **17**, 2195 (1984).
  - [12] M. B. Shah, D. S. Elliott, P. McCallion, and H. B. Gilbody, *J. Phys. B* **21**, 2751 (1988).
  - [13] M. S. Pindzola and F. J. Robicheaux, *Phys. Rev. A* **61**, 052707 (2000).
  - [14] A. J. Murray and F. Read, *J. Phys. B* **26**, L359 (1993).
  - [15] I. Bray, D. V. Fursa, J. Röder, and H. Erhardt, *J. Phys. B* **30**, L101 (1997).
  - [16] S. Rioual, J. Röder, B. Rouvellou, H. Erhardt, A. Pochat, I. Bray, and D. V. Fursa, *J. Phys. B* **31**, 3117 (1998).
  - [17] A. T. Stelbovics, I. Bray, D. V. Fursa, and K. Bartschat, *Phys. Rev. A* **71**, 052716 (2005).
  - [18] E. Schow, K. Hazlett, J. G. Childers, C. Medina, G. Vitug, I. Bray, D. V. Fursa, and M. A. Khakoo, *Phys. Rev. A* **72**, 062717 (2005).
  - [19] M. S. Pindzola, F. J. Robicheaux, J. P. Colgan, M. C. Witthoef, and J. A. Ludlow, *Phys. Rev. A* **70**, 032705 (2004).
  - [20] R. D. Cowan, *The Theory of Atomic Structure and Spectra* (University of California Press, Berkeley, 1981).